Chemical Engineering Journal 151 (2009) 372–379

Contents lists available at ScienceDirect

Chemical Engineering Journal

journal homepage: www.elsevier.com/locate/cej

Rhodium colloidal suspension deposition on porous silica particles by dry impregnation: Study of the influence of the reaction conditions on nanoparticles location and dispersion and catalytic reactivity

L. Barthe[a,*], M. Hemati[a], K. Philippot[b], B. Chaudret[b], A. Denicourt-nowicki[c], A. Roucoux[c]

[a] Laboratoire de Génie Chimique – UMR CNRS 5503 – INP-ENSIACET, 5 rue Paulin Talabot, BP 1301, 31106 Toulouse cedex 01, France
[b] Laboratoire de Chimie de Coordination – UPR CNRS 8241, 205 route de Narbonne, 31077 Toulouse cedex 04, France
[c] Ecole Nationale Supérieure de Chimie de Rennes, CNRS, UMR 6226, Avenue du Général Leclerc, CS 50837, 35708 Rennes Cedex 7, France

ARTICLE INFO

Article history:
Received 31 July 2008
Received in revised form 26 March 2009
Accepted 30 March 2009

Keywords:
Rhodium nanoparticles
Colloidal suspension
Dry impregnation
Operating conditions
Supported catalysts
Aromatic compounds
Hydrogenation

ABSTRACT

Rhodium composite nanomaterials were synthesized by an innovating process called dry impregnation in a fluidized bed. It consists in spraying an aqueous colloidal suspension of rhodium on silica porous particles. The use of this precursor solution containing preformed nanoparticles avoids calcination/activation step.

Different composite nanomaterials were prepared displaying various metal loadings. The operating conditions were tuned to modify τ_s, the solvent vapour saturation rate value, in order to influence the deposit location: either uniform on the whole silica particles or at the particles surface like a coating. τ_s is defined as the ratio between solvent content in the bed atmosphere and the maximum solvent content.

The obtained samples were investigated in catalytic hydrogenation of aromatic compounds under very mild conditions. Their catalytic performances were compared to those of the original colloidal suspension in one hand and of a similar catalyst prepared through wet impregnation in another hand. Interesting activity and selectivity were observed.

This illustrates the interest of the dry impregnation method: this way allows an easy control of the metal loading as well as of the metal loading location in the support particles. Moreover, the support particle size and morphology are preserved.

1. Introduction

The interest in metal nanoparticles for applications in catalysis is now well-known [1–4] and mainly results from their high specific surface area due to their small size giving rise to high active sites numbers. Metal nanoparticles are generally considered as species at the frontier between homogeneous and heterogeneous catalysts. From this particular matter state, catalytic specificities, which are not offered by classical catalysts, could be expected and several systems are now available in the literature illustrating their particular behaviour [5–7].

The preparation of metallic nanospecies in liquid-phase is possible through various chemical syntheses and the reduction of metal salts in aqueous media is one of the most known methods [8]. For example, colloidal suspensions of rhodium can be prepared by chemical reduction of $RhCl_3$ and stabilized by highly hydrosoluble quaternary ammonium salts and they have proved to be active catalysts for hydrogenation of various aromatic compounds [9]. Nevertheless, colloidal suspensions display some disadvantages as their lack of stability at elevated temperatures (agglomeration is often observed at temperature higher than 100 °C) or their recycling with soluble products. It appears then clearly that the deposition of metal nanoparticles onto a support would circumvent these drawbacks and afford the advantages of traditional supported catalysts. The way followed to prepare supported nanocatalysts is generally the wet impregnation method [10]. It consists in the immersion of the chosen support in a colloidal suspension under stirring to favour the diffusion of the nanoparticles inside the support grains. This technique is easy to carry out but can present some weak points such as: loss of precursor, reduction of the support particle size (most of the porous supports, prepared by sol–gel process, disaggregate in solution under stirring) and dependence of the deposit location on the physico-chemical properties of the solution-support couple.

Taking into account these different points, the preparation of supported catalysts following a dry impregnation method appears as an interesting alternative technique. The preparation of

* Corresponding author.
E-mail addresses: Laurie.Barthe@ensiacet.fr (L. Barthe), Mehrdji.Hemati@ensiacet.fr (M. Hemati).

1385-8947/$ – see front matter © 2009 Elsevier B.V. All rights reserved.
doi:10.1016/j.cej.2009.03.051

composite nanomaterials by dry impregnation in a fluidized bed has been developed by [11]. Its principle consists in spraying a solution containing a metal source into a hot fluidized bed of porous fine particles. After the impregnation step, metallic precursor decomposition and/or activation can be performed in the same apparatus. Up to now, this technique has been successfully applied using solutions of metal salts (iron, manganese and copper nitrate) or organometallic complexes (bis(dibenzylidene)palladium, $[Pd(dba)_2]$ or palladium allyl chloride $[PdCl(allyl)]_2$) as metal sources. Most particularly, the deposition of metal salts gave rise to interesting composite nanomaterials displaying catalytic properties [12].

This dry impregnation technique offers several advantages. For example, the whole sprayed metal precursor is deposited and the metal loading is thus controlled by the impregnation time. Moreover the initial size of support grains is conserved. But, its major advantage concerns the deposit location that can be oriented depending on the targeted composite nanomaterials [12,13]. Indeed, previous works with metal complexes showed that a competition between two phenomena, the drying and the capillarity, controls the deposit location. An adequate choice of operating conditions (bed temperature, liquid and fluidization gas flow rate), otherwise the appropriated values of τ_s, the solvent vapour saturation rate, and IM, the impregnation module, permit to predict the deposit location. τ_s is defined as the ration the ratio between solvent content in the bed atmosphere and the maximum solvent content. IM is defined as the ratio between a drying characteristic time, t_{dry}, and a capillary penetration time, t_{cap}.

t_{cap}, the time necessary for liquid penetration in the pores, can be estimated from the following equation taken from the model of the parallel capillary beam [14]:

$$t_{cap} = \frac{2\mu x^2}{\gamma_{LV} \cos\theta r_{pore}} \quad (1)$$

where μ is the liquid viscosity, x the pore length equivalent to the radius particle multiplied by the tortuosity factor, γ_{LV} the interfacial tension, θ the contact angle and r_{pore} the pore radius.

t_{dry}, the time necessary for a particle saturated by pure solvent to be transformed into a dry particle under defined fluidized bed conditions (temperature and humidity). The calculation of this characteristic time is based on the mass and energy balances on a single wetted particle considering that the mass transfer is controlled by external resistance (gas phase). The model's equations described in previous works [13,15] lead to this last equation:

$$t_{dry} = \frac{d_p \chi \rho_s}{6k_y(Y_i - \bar{Y})} \quad (2)$$

where d_p is the particle diameter, χ the internal support porosity, ρ_s the solvent density, k_y the overall mass transfer coefficient, $\bar{Y}$ the average solvent content in the bed atmosphere determined by overall mass balance on the reactor, and Y_i the absolute solvent content at the interface (depending on the particle temperature and humidity [13]).

According to these two parameters, homogeneous deposit of nanoparticles is located inside or at external surface of the support. For example, in the case of dry impregnation of fine silica particles by an iron nitrate aqueous solution, our experimental results show that soft drying conditions ($\tau_s \geq 0.2$ and IM ≥ 30) lead to a homogeneous deposit while under fast drying conditions ($\tau_s < 0.2$ and IM < 30), the deposit is located at the particle external surface.

After these findings, a new challenge for us consisted in the use of aqueous colloidal solutions containing preformed metal nanoparticles to check the applicability of our process to another metal source. This approach using metallic nanospecies could be promising since it avoids thus the necessary step of decomposition/activation of metal complexes. Nevertheless, this project was ambitious because no deposition of colloidal solution was known in the literature and this could present some technical difficulties.

This paper describes the dry impregnation of fine porous silica particles by a rhodium colloidal suspension. The so-prepared samples were characterised to follow the impregnation kinetics and check the metal deposit location. Finally, the activity of these composite nanomaterials was compared to that of colloidal suspension on one hand and to that of similar catalysts prepared with the same materials (colloidal suspension and support) by classical wet impregnation on the other hand.

2. Methods and materials

2.1. Starting materials

2.1.1. Metal source

Rhodium chloride hydrate was obtained from Strem Chemicals. Sodium borohydride and all aromatic substrates were purchased from Aldrich or Fluka and were used without further purification. Water was distilled twice before use by conventional method. The surfactant HEA-16Cl was prepared as previously described in the literature [16].

2.1.2. Solid supports

Fine porous silica particles of two different sizes but with similar physical properties were used as catalysts support (silica gel Merck 60). Their average pore diameter was 5.5 nm. Their other physical and hydrodynamic characteristics are listed in Table 1.

2.2. Experimental procedures

2.2.1. Preparation of rhodium colloidal suspensions

The rhodium colloidal aqueous suspensions containing rhodium (0) nanoparticles were prepared as previously described (Fig. 1a) [17]. More precisely, sodium borohydride (36 mg, 9.5×10^{-4} mol) was added to an aqueous solution of N,N-dimethyl-N-cetyl-N-(2-HydroxyEthyl)Ammonium chloride salts, namely HEA16Cl (95 mL, 7.6×10^{-3} mol L^{-1}). This solution was quickly added under vigorous stirring to an aqueous solution of the precursor $RhCl_3.3H_2O$ (100 mg, 3.8×10^{-4} mol). The initial red solution darkened immediately, proving the formation of the aqueous Rh(0) colloidal suspension. Transmission Electron Microscopy (TEM) images revealed well-dispersed rhodium nanoparticles (Fig. 1b) with a mean size of 2.4 nm (Fig. 1c). It was verified that such colloidal solutions are stable for several months at room temperature.

2.2.2. Preparation of supported nanoparticles by dry impregnation in fluidized bed (Dry Imp catalysts)

The experiments were carried out in a batch fluidized bed, allowing syntheses under controlled atmosphere (inert or reductive) depending on the metal precursor nature. The reactor is a stainless steel conical column with a 30 mm base diameter, a 112 mm top diameter and 300 mm in height (Fig. 2). Its dimensions make it possible to reduce the metal precursor consumption and the impregnation time since it operates at laboratory scale (production

Table 1
Physical and hydrodynamic characteristics of the silica particles used as supports.

Characteristics	Si 120	Si 80
Mean diameter d_p (μm)	120	80
Pore diameter d_{pore} (nm)	5.5	5.4
Specific surfaces S_{bet} (m^2/g)	530	490
Pore volume V_p (cm^3/g)	0.81	0.77
Internal porosity χ (%)	60	58
U_{mf} at 25 °C (minimum fluidization velocity) (m/s)	0.0035	0.0022
U_t at 25 °C (terminal velocity) (m/s)	0.23	0.15

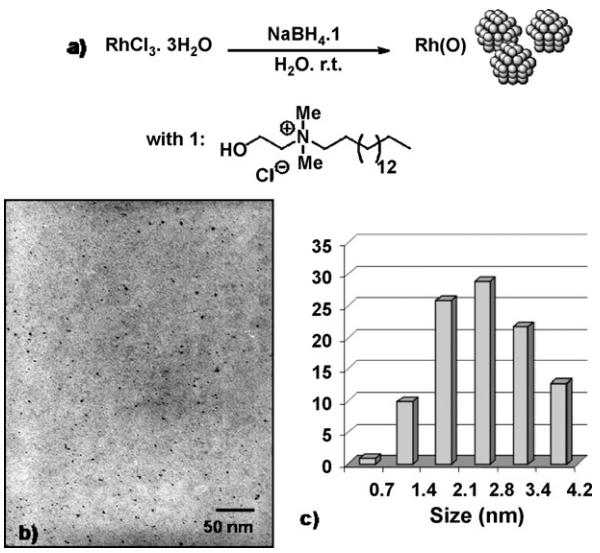

Fig. 1. (a) Preparation of surfactant-stabilized Rh(0) nanoparticles, (b) TEM observations of the colloidal suspension and (c) nanoparticles size distribution.

of catalyst: 30 to 100 g). The gas distribution at the column base is ensured by a stainless steel perforated plate with a porosity of 0.5% (12 holes of 1 mm, organized according to a triangular mesh of 5 mm). Before entering the bed, the fluidizing gas flow rate is measured by a rotameter and preheated by an electrical heater. The bed temperature is controlled by means of a PID regulator which commands the furnace heating power. At the outlet of the column, the elutriated particles are separated from the gas phase by a cyclone.

The impregnating solutions are placed into two reservoirs, one containing pure solvent for experiment starting, and the second containing the metallic precursor solution. The solution is drawn up by a volumetric pump from a reservoir to a spray nozzle. The atomizer is a downward facing nozzle and is located in the bed. Temperature and pressure drop monitoring is achieved throughout all the impregnation.

The general experimental protocol is as follows:

- The column is initially charged with a given mass of porous silica particles.
- The powder is fluidized by a fixed hot gas flow rate.
- The pure solvent (water in the present case) is sprayed within the bed, at the same flow rate as the colloidal suspension.
- As soon as the bed temperature is stabilized, the solvent is replaced by the solution containing metallic nanoparticles.

For all the experiments carried out, the solution flow rate (50 g/h) and the support mass (30 g) were maintained constant. The fluidization gas flow rate is adjusted according to the particles diameter (0.8 m^3/h when d_p = 120 μm and 0.6 m^3/h when d_p = 80 μm). It should be noted that the selected gas flow rate is about 10 times the minimum fluidization velocity at 25 °C. For each experiment, the bed temperature, the final metal loading, τ_s and IM are presented in Table 2.

A study of the impregnation kinetics can be obtained from experiments 1 to 4. The influence of the bed temperature parameter on the rhodium nanoparticles dispersion in the porous silica particles can be studied considering experiments 3 and 5 while the support particle size effect can be determined from experiments 3 and 6.

2.2.3. Catalytic tests: hydrogenation of arenes

Catalytic reactions were carried out under mild conditions (ambient temperature, 1 atm of H_2). A 25 mL round bottom flask, charged with silica-supported Rh(0) catalyst (1 g, 10 mL solvent) and the appropriate aromatic substrate ([substrate]/[Rh] = 100), is connected to a gas burette (500 mL) with a flask to balance pressure. Then, the system is filled with hydrogen and the mixture is magnetically stirred at 1500 min^{-1}. The reaction is monitored by gas chromatography analyses.

2.3. Characterization methods

To determine the textural properties of the different samples obtained after impregnation of silica particles with colloidal rhodium suspension, various characterization techniques were

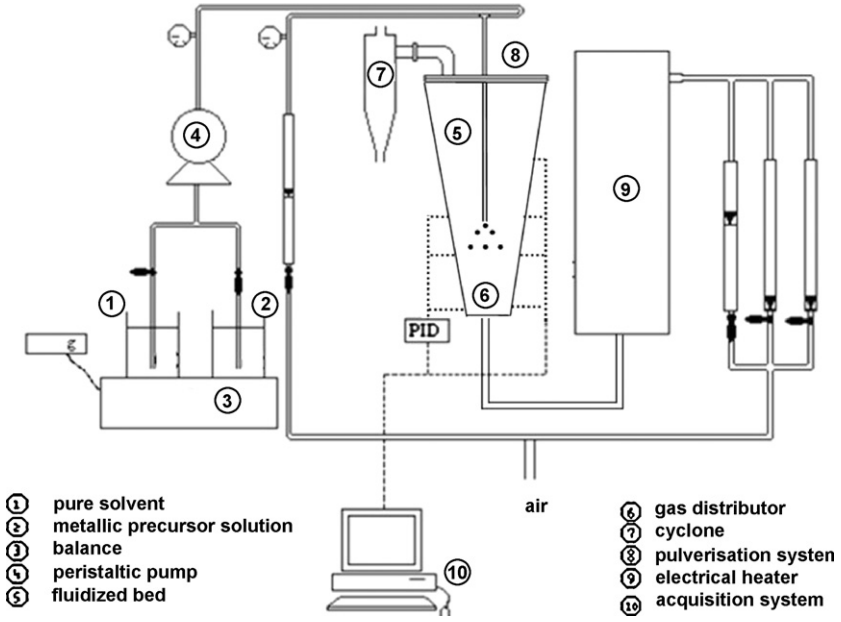

Fig. 2. Experimental set up for rhodium nanoparticles deposition by dry impregnation.

Table 2
Operating conditions used for the preparation of supported rhodium nanoparticles by Dry Impregnation in fluidized bed.

Dry Impregnation samples	Particle diameter d_p (μm)	Bed temperature T_{bed} (°C)	Impregnation time (min)	Final metal loading (%)	τ_s	IM
Dry Imp 1	120	45	23	0.02	0.77	400
Dry Imp 2	120	45	43	0.04	0.77	400
Dry Imp 3	120	45	108	0.08	0.77	400
Dry Imp 4	120	45	156	0.16	0.77	400
Dry Imp 5	120	106	108	0.08	0.01	28
Dry Imp 6	80	51	108	0.08	0.76	400

Table 3
Theoretical and experimental rhodium loadings for Dry Impregnation catalysts 1 to 4.

	Dry Imp 1	Dry Imp 2	Dry Imp 3	Dry Imp 4
Theoretical rhodium loading (%)	0.02	0.04	0.08	0.16
Experimental rhodium loading (%)	0.015	0.035	0.08	0.15

used such as:

- Laser granulometry (particles mean diameter and size distribution),
- Helium pycnometry (apparent and real bulk density),
- Mercury porosimetry (pore volume),
- N_2 adsorption–desorption (BET specific surface and pores size distribution),
- Transmission electron microscopy (TEM) (topology of the catalysts and metal nanoparticles size)
- Elemental analysis for metal content determination (metal loading).

3. Results and discussion

We have studied the influence of various parameters on the morphological characteristics and the catalytic properties of solids obtained through dry impregnation.

3.1. Morphological characteristics of the samples prepared by dry impregnation (Dry Imp catalysts)

3.1.1. Kinetic study

Experiments 1 to 4 were carried out using different impregnation times and constitute thus a kinetic study.

The first observation concerns the colour of the obtained composite materials which is grey. Since silica particles have a white colour and the colloidal suspension a black one, this grey colour evidences that a metal deposit took place in the support grains. To confirm that the whole sprayed rhodium nanoparticles were deposited within the support, the solid metal loading was determined for all samples. The results are gathered and compared with the theoretical values in Table 3.

The results show that the experimental loadings obtained are very close to the expected theoretical values. It thus appears that all the sprayed colloidal suspension was deposited in the support. There is no metal loss. Therefore, at a given precursor concentration, the spraying time determines the metal loading.

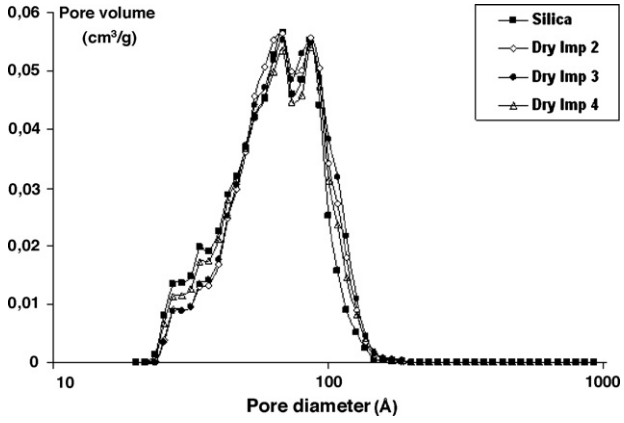

Fig. 3. Pore size distributions obtained for pure silica and Dry Impregnation catalysts 2 to 4.

Two parameters could be controlled during the catalyst preparation. The impregnation module, IM, is defined as the ratio between a drying time and a capillary penetration time. A solvent vapour saturation rate is also considered, τ_s, defined as the ratio between solvent content in the bed atmosphere and the maximum solvent content. The experimental results show that soft drying conditions ($\tau_s \geq 0.2$ and IM ≥ 30) lead to a homogeneous deposit inside the support particles while under fast drying conditions ($\tau_s < 0.2$ and IM < 30), the deposit is located at the particle external surface.

For experiments 1 to 4, the solvent vapour saturation rate τ_s is equal to $0.77 > 0.2$ and the Impregnation Module IM is equal to $400 > 30$, favouring an uniform deposit inside the support particles. To check that deposited nanoparticles are well dispersed on all the support grains volume and that they remained individual (no agglomeration), the samples were analyzed by granulometry. It appears that the average diameter of the silica particles remains the same and does not increase during the deposit. This indicates that no agglomeration phenomenon took place. However, the quantity of added metal being rather weak, it may be not detected by granulometry that make it impossible to conclude on the deposit location. It was thus necessary to use other techniques.

The porosity of the four catalysts has then been determined. In spite of the small quantity of deposited rhodium, the results presented in Table 4 show a tendency towards a reduction of the specific surface (from 500 to 485 m^2/g) and pore volume (from 0.81 to 0.75 cm^3/g). This leads to think that the metal deposit was carried out in a homogeneous way within the silica grains.

This hypothesis was confirmed by analysing the evolution of the pore size distribution for each rhodium loading (Fig. 3). The pattern is not modified and the curves are very close.

Table 4
Physical properties of the virgin support and Dry Impregnation catalysts 1 to 4.

	Silica	Dry Imp 1	Dry Imp 2	Dry Imp 3	Dry Imp 4
Experimental rhodium loading (%)	0	0.015	0.035	0.08	0.15
Specific surface S_{bet} (m^2/g)	500	498	493	488	485
Pore volume V_p (cm^3/g)	0.81	0.80	0.79	0.77	0.75

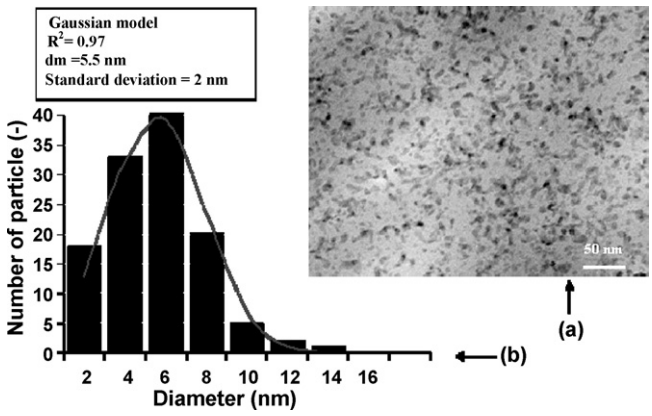

Fig. 4. (a) TEM micrograph (magnification: 200,000); (b) nanoparticles size distribution for Dry Impregnation catalyst 3.

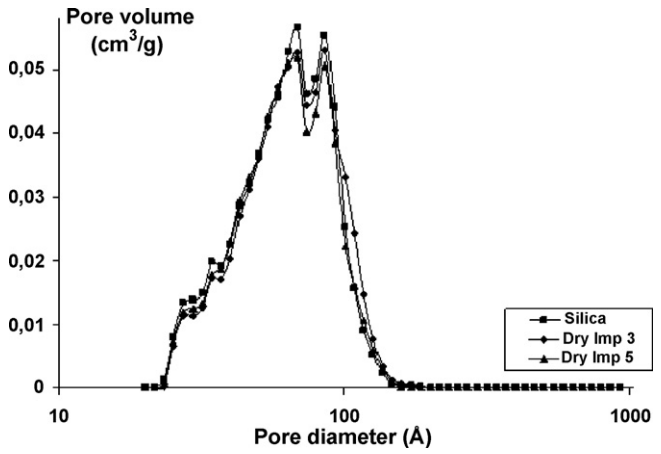

Fig. 5. Pore size distributions obtained for pure silica and Dry Impregnation catalysts 3 and 5.

The different samples have also been observed by Transmission Electronic Microscopy after ultramicrotomy preparation to check rhodium nanoparticles dispersion. The analysis of various silica particles regions showed rhodium nanoparticles homogeneously dispersed in the support (Fig. 4a). From TEM micrographs we could also determine the rhodium nanoparticles size distribution and their mean diameter by manual counting (Fig. 4b). The size distribution can be represented by a Gaussian model and the rhodium nanoparticles mean size is 5.5 nm (standard deviation 2 nm). After deposition, the rhodium nanoparticles have an average size of around 5.5 nm corresponding to the silica pore average diameter (5.5 nm). It seems thus that the pore diameter controls the nanoparticles maximum size.

3.1.2. Deposit location

The influence of the temperature of the fluidized bed on rhodium nanoparticles dispersion in the porous support was studied from experiments 3 and 5. The same colloidal suspension quantity was sprayed for these two experiments, but during experiment 5 the values of τ_s and IM were reduced to obtain a deposit on the silica particles surface, like a coating. So, the fluidized bed temperature was increased from 45 to 106 °C, which reduces τ_s from 0.77 to 0.01 and IM from 400 to 28 (Table 2).

The samples obtained were analysed by elemental analysis. The experimental rhodium loadings are very close to the expected theoretical values. This confirms the good deposit efficiency.

A granulometry analysis was carried out on the two solids. The average diameter of the silica particles is quite the same for the two samples, the difference being not significant. This result was expected as the deposit thickness at the particle surface would not exceed 1 μm.

The porosities of the samples were also determined and compared. The pore size distribution pattern is similar for the two products and also close to the one of the virgin support (Fig. 5). For the two impregnated solids, a very light reduction of the porosity was observed, slightly more pronounced in the case of experiment 5 corresponding to τ_s and IM weak.

This is confirmed by the observation of a low reduction in pore volume. In the same way, the specific surface decreases in a more significant way when τ_s and IM are weak.

The different samples were also observed by Transmission Electronic Microscopy after ultramicrotomy preparation to check rhodium nanoparticles dispersion. Sample 3 has been previously described (see kinetic study and Fig. 4) for which a uniform dispersion of the rhodium nanoparticles in the silica support was observed. Concerning Sample 5, at low magnification (×10,000), a dark zone has been observed on all silica particle circumference, Fig. 6a. Thus in this case, the deposit took place on the silica particles surface, forming a coating of approximately 500 nm thickness. This was confirmed at higher magnification (×100,000), Fig. 6b. The nanoparticles detected on the silica particles surface are individual nanoparticles (diameter around 5 nm), or assembled into small agglomerates (size around 30 nm). No rhodium nanoparticles were detected in the core of the silica grains.

3.1.3. Support particles size

The effect of the size of the silica particles can be determined comparing experiments 3 and 6. The same operating conditions were followed in these two experiments, using supports presenting the same characteristics (specific surface, pore volume, pore

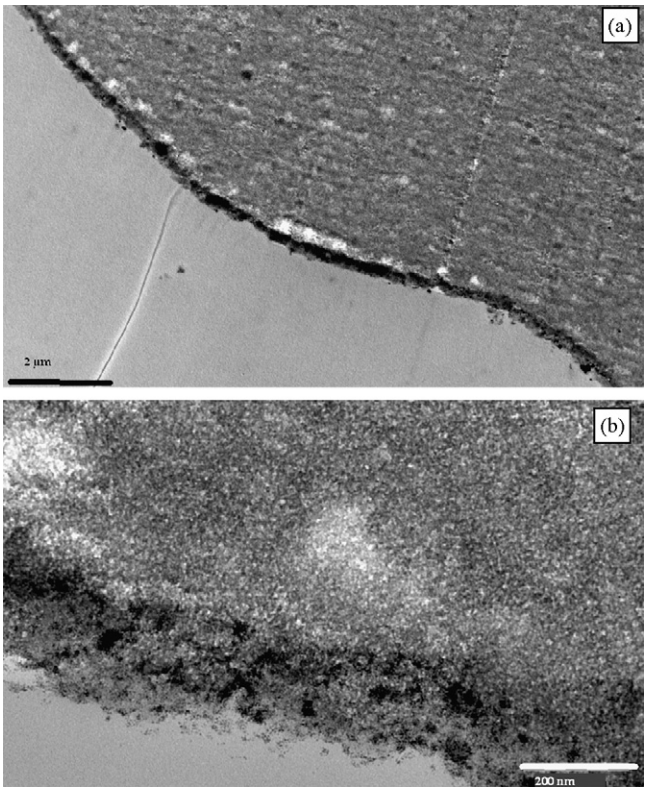

Fig. 6. TEM micrographs for Dry Impregnation catalyst 3 (a) magnification 10,000 and (b) magnification 100,000.

diameter) but having different particle diameters (respectively 120 and 80 μm).

The silica particles being finer, we had to decrease the fluidization gas flow rate to get satisfying fluidization regime. This led to a reduction of heating by the gas used for solvent evaporation. To circumvent this lack, the temperature of the inlet gas and consequently the bed one were increased, to maintain τ_s and IM at the previous value.

The obtained product, Sample 6, was characterized by the same techniques as those previously used. Results were perfectly identical to those obtained for Sample 3:

- All the metal sprayed is deposited. The operation efficiency is about 100%.
- The silica particles diameter is not affected significantly by rhodium nanoparticles deposit.
- Specific surface and pore volume decrease very slightly compared to virgin support.
- The pore size distribution pattern is the same before and after deposit.
- The TEM micrograph after ultramicrotomy revealed a good dispersion of the rhodium nanoparticles in the support grains.
- The detected rhodium nanoparticle average size is around 5.5 nm.

Taking into account all these results, it appears that the support particle size modification (between 80 and 120 μm) does not affect the rhodium nanoparticles deposit.

In conclusion of this part, we can say that the dry impregnation technique is very flexible. First, the metal loading can be fixed by the spraying time. Secondly, the deposit location can be oriented by choosing correctly the operating conditions: the metal deposit can be either only at the surface of the support particles like a coating or homogeneously distributed on the whole particle volume. Finally, the support particle size and morphology are preserved and the silica particles pore diameter controls the nanoparticle maximal size. The choice of the support is thus very important, at least in the case of silica gel.

3.2. Investigation in catalytic hydrogenation of aromatic compounds

The rhodium based composite nanomaterials prepared by dry impregnation in a fluidized bed (Dry Imp catalysts) as previously described have been tested in catalysis. The hydrogenation of aromatic compounds has been chosen to evaluate these catalysts in terms of catalytic performances in comparison with the original colloidal suspension [16] and with similar catalysts obtained by wet impregnation method [10]. For that purpose, several parameters have been evaluated in the hydrogenation of toluene as model substrate. Then, based on optimized conditions, alkylated, functionalized and disubstituted substrates have been studied to check efficiencies of Dry Imp catalysts.

3.2.1. Comparison of catalytic performances of rhodium colloidal suspension, Wet Imp and Dry Imp catalysts in toluene hydrogenation

The performances of a Dry Imp catalyst have been investigated in toluene hydrogenation reaction in aqueous phase and compared to those of colloidal rhodium suspension [16] and a Wet Imp catalyst [10] already known. For this study, the selected catalyst is the solid Dry Imp 3, which presents the same rhodium content as the catalyst prepared by wet impregnation as well as that of the colloidal suspension. The results are reported in Table 5.

This comparison evidences that higher activities are obtained with supported catalysts: a total conversion is obtained in 2.25 h and 2.5 h respectively with Dry Imp and Wet Imp catalysts against 3.6 h with the colloidal suspension. In addition, the Dry Imp catalyst is slightly more active than the Wet Imp one. These findings show that the diffusion phenomenon in the solid is not the limitation step in reaction process.

Table 5
Toluene hydrogenation in aqueous phase by various catalytic systems (Dry Impregnation Catalyst 3, Wet Impregnation Catalyst and the colloidal suspension)[a].

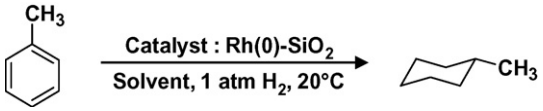

Entry	Catalyst[b]	Time (h)	Conversion rate[c](%)	TOF[d] (h^{-1})
1	Dry Imp 3	2.25	100	167
2	Wet Imp	2.5	100	150
3	Rh-HEA16Cl suspension	3.6	100	83

[a] Conditions: Catalyst Rh-SiO_2 (1 g, 0.08 wt% Rh), toluene, [S]/[M] = 100, 10 mL H_2O, 1 atm H_2, RT.
[b] Dry Imp and catalyst s prepared according to dry impregnation approach. Rh-HEA16Cl suspension and Wet Imp catalysts prepared as described previously.
[c] Determined by GC analysis.
[d] Turnover frequency defined as mol of H_2 per mol of rhodium per hour.

Moreover, these results highlight the interest to deposit the rhodium nanoparticles on a support to enhance their catalytic properties. This deposition probably permits to avoid their aggregation. Moreover, the catalyst recuperation is easier in this case.

3.2.2. Investigation of Dry Impregnation catalysts in various reaction conditions and other substrates hydrogenation

3.2.2.1. Effect of the solvent. The influence of various solvents (water, hexane, dichloromethane) has been investigated in the hydrogenation of toluene. The results obtained with Dry Imp 3 catalyst are summarized in Table 6.

Dry Imp catalyst shows a slow catalytic activity in dichloromethane since only 27–33% conversion is obtained in 5.5 h (Entry 3). However, as already reported in previous works with the Wet Imp, [10], total conversion in water has been achieved with quite interesting Turnover Frequency (TOF) of 167 h^{-1} (Entry 2). Finally, the best catalytic activity has been reached in hexane with total conversion in methylcyclohexane (TOF of 282 h^{-1}) with Dry Imp (Entry 1).

The difference of catalytic activity observed in hexane and water may be explained by a better solubilisation of the substrate in hexane and thus a better diffusion of the substrate to the metallic species inside the support grains. It could be attributed to the surface quality of the catalysts grains and their affinity with hexane.

3.2.2.2. Catalyst recycling. We have also investigated the recycling of the silica-supported nanoparticles, which constitutes one of the main advantages of supported catalysts, in toluene hydrogenation in hexane at 20 °C and 1 atm H_2. The catalyst was easily recovered after each run by simple filtration and dried at 60 °C before another

Table 6
Toluene hydrogenation by Dry Impregnation catalyst 3 in various solvents[a].

Entry	Catalyst[b]	Solvent nature	Time (h)	Conversion rate[c](%)	TOF[d] (h^{-1})
1	Dry Imp 3	Hexane	1.33	100	282
2	Dry Imp 3	Water	2.25	100	167
3	Dry Imp 3	Dichloromethane	5.5	27	18

[a] Conditions: Catalyst Rh-SiO_2 (1 g, 0.08 wt% Rh), toluene, [S]/[M] = 100, 10 mL solvent, 1 atm H_2, RT.
[b] Dry Imp catalyst prepared according to dry impregnation approach.
[c] Determined by GC analysis.
[d] Turnover frequency defined as mol of H_2 per mol of rhodium per hour.

Table 7
Hydrogenation of toluene by catalysts prepared by Dry Impregnation on various sized silica and with various deposit location[a].

Entry	Catalyst[b]	Silica particle diameter (μm)	Deposit location	Time (h)	Conversion[c] (%)	TOF[d] (h^{-1})
1	Dry Imp	80	Uniform	1.33	94	265
2	Dry Imp 3	120	Uniform	1.33	100	282
3	Dry Imp 5	120	At the surface	1.33	100	282

[a] Conditions: Catalyst Rh-SiO_2 (1 g, 0.08 wt% Rh), toluene, [S]/[M] = 100, 10 mL hexane, 1 atm H_2, RT.
[b] Dry Imp catalyst prepared according to dry impregnation approach.
[c] Determined by GC analysis.
[d] Turnover frequency defined as mol of H_2 per mol of rhodium per hour.

run with a new addition of substrate. The kinetics of the two runs are presented on Fig. 7, using Dry Imp catalyst.

The two runs present the same kinetics curves. However, the reaction is slightly slower in the second run with a complete conversion in methylcyclohexane after 90 min, compared to 80 min for the first run. This slight fall in catalytic activity could be related to a rhodium loss during recycling. However, elemental analysis of Dry Imp catalyst has proved that the metal loading remains the same between the two runs. Another explanation could rely on the filtration step. To justify this hypothesis, we have reloaded the reaction mixture with the same quantity of substrate (toluene) at the end of the first catalytic run. For two consecutive tests performed with Dry Imp catalyst, we have observed the same catalytic activity (complete conversion in 80 min), and thus no loss of activity between the different runs. It is important to notice that this refill protocol is very used in industry.

3.2.2.3. Effect of the support and of deposit location. We have first investigated the effect of the support, thus modifying the grains size of catalysts. Two kinds of silica have been evaluated: the classical one, which has been used for all the previous experiments, with a particle diameter of 120 μm and a finer one, possessing a diameter of 80 μm. The two catalysts have been tested in toluene hydrogenation in hexane, under standard conditions (1 bar H_2 and RT). The results are given in Table 7.

It appears that the grains size of the two tested silica has no significant influence on catalytic performances since TOFs (Turnover Frequency) are quite similar. These results confirm again that the diffusion process is not the limitation factor in our operating conditions.

It should be noted that the catalysts particles desagglomerate in solution during the catalysis. So the support particle size can not really be studied in the application. This size reduction of the support grains could be explained by the silica preparation. It's a material presenting a pellet-grains morphology formed by small particles agglomerates [18]. It appears that, in solution and under stirring, the particles desagglomerate due to low cohesion forces.

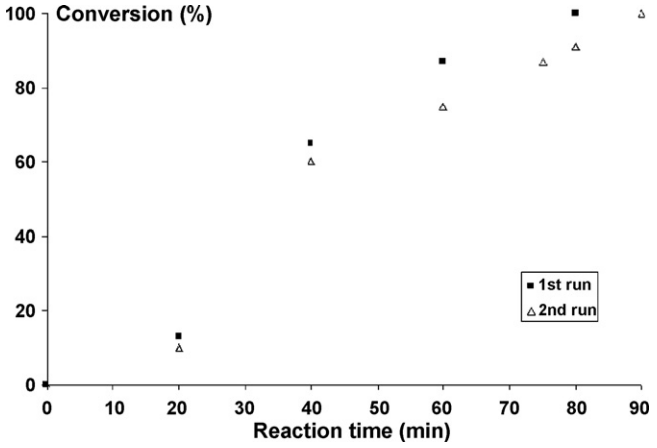

Fig. 7. Recycling of Dry Impregnation catalyst in toluene hydrogenation in hexane.

As previously mentioned, the interest in using dry impregnation method is the possibility to orient the deposit location. In that context, the influence of the rhodium nanoparticles location on toluene hydrogenation has also been studied, comparing the activity of two catalysts having different metal location (Dry Imp 3 and Dry Imp 5). Dry Imp 3 displays an uniform distribution of metal nanoparticles in the support, whereas Dry Imp 5 possesses at the silica particle surface a coat of approximately 500 nm constituted by rhodium nanoparticles. The results are reported in Table 7.

As expected, these tests reveal that the deposit location has a weak influence on the catalytic activity: the results are similar whatever the deposit location is. Whatever the location of metal is, all rhodium becomes accessible. This would explain why the same catalytic activities are obtained.

3.2.2.4. Effect of the rhodium loading. Dry Imp catalysts with different rhodium loadings have been prepared and evaluated in toluene hydrogenation in hexane using the standard conditions and a substrate/metal ratio of 100. The results are reported in Table 8.

These experiments highlight that the catalytic activity increases with the increase in rhodium loading. At very low rhodium loadings (Entries 1 and 2), very low conversions between 4 to 39% are obtained in 2.75 h. However, at higher metal loadings (Entries 3 and 4), the toluene is totally converted in methylcyclohexane in less than 1.33 h. We could presume that all the deposited rhodium is active and accessible to the substrate.

3.2.2.5. Hydrogenation of various aromatic derivatives. The performances of Dry Imp catalysts have been investigated in the hydrogenation reactions of monofunctionalized and disubstituted arene derivatives, such as toluene, anisole and *o*-xylene, respectively. All the tests were carried out in hexane under standard conditions (1 bar H_2, RT). The results are presented in Table 9.

In all cases a complete conversion of the substrate in the totally hydrogenated compound has been observed. Moreover, the hydrogenation of *o*-xylene (Entry 3) leads to the formation of 1,2-dimethylcyclohexane with a 92/8 *cis/trans* ratio. This result has already been reported in the literature for aqueous

Table 8
Influence of rhodium loading of Dry Impregnation Catalysts in toluene hydrogenation[a].

Entry	Catalyst[b]	Rhodium loading (%)	Time (h)	Conversion[c] (%)
1	Dry Imp 1	0.015	2.75	4
2	Dry Imp 2	0.035	2.75	39
3	Dry Imp 3	0.08	1.33	100
4	Dry Imp 4	0.15	1	100

[a] Conditions: Catalyst Rh-SiO_2 (1 g), toluene, [S]/[M] = 100, 10 mL hexane, 1 atm H_2, RT.
[b] Dry Imp catalysts according to the dry impregnation method.
[c] Determined by GC analysis.

Table 9
Hydrogenation of various substrates by Dry Impregnation Catalyst[a].

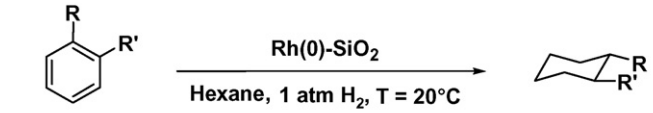

R = CH_3, OCH_3
R' =H, CH_3

Toluene : R = CH_3 and R' = H; Anisole : R = OCH_3 and R' = H; Orthoxylene R = R' = CH_3 .

Entry	Substrate	Catalyst[b]	Time (h)	Conversion[c] (%)	TOF[d] (h^{-1})
1	Toluene	Dry Imp 3	1.33	100	282
2	Anisole	Dry Imp 3	1.25	100	300
3	o-Xylene	Dry Imp 3	3.33	94 (cis/trans = 92/8)	120

[a] Conditions: Catalyst Rh-SiO_2 (1 g, 0.08 wt% Rh), toluene, [S]/[M] = 100, 10 mL hexane, 1 atm H_2, RT.
[b] Dry Imp catalysts according to the approach dry impregnation.
[c] Determined by GC analysis.
[d] Turnover frequency defined as mol of H_2 per mol of rhodium per hour.

HEA16Cl-stabilized Rh(0) colloidal suspensions [17] and also for nanoparticles inserted into mesoporous siliceous materials [19].

4. Conclusion

The deposit of a rhodium colloidal suspension on porous silica particles by the dry impregnation technique in a fluidized bed was carried out successfully. The kinetic study of the impregnation revealed that the deposit of the colloidal suspension presents the same behaviour as that of a metal salt: the operation efficiency is about 100%, the impregnation time controls the metal loading and the deposited nanoparticles maximal size is controlled by the matrix pores diameter. The deposit location can be chosen, by fixing the value of τ_s. A value of $\tau_s < 0.2$ led to the silica particles coating by rhodium nanoparticules while a value included between 0.2 and 0.8 permit to obtain a uniform deposit.

The prepared and characterized composite materials were tested in catalysis of aromatic compounds hydrogenation, interesting reaction at the economic as well as environmental levels. We could note that the solids prepared by dry impregnation in a fluidized bed are active under very soft conditions. They present catalytic performances equivalent to those of catalysts prepared in a traditional way but higher than those of the corresponding colloidal suspension. Hydrogenation of compounds such as toluene, anisole and orthoxylene were carried out with good conversions and an interesting selectivity for the last substrate. The various catalytic tests permit to conclude that for these aromatic compounds, hexane is the better solvent and the consecutive refills lead to the same performance. The rhodium loading is a key parameter whereas the deposit location is not very important for these tested reactions as the catalysts particles desagglomerate in solution under stirring.

Indeed, to obtain a dry catalyst this catalyst preparation technique presents several advantages such as: (1) the support particles morphology and size are preserved, (2) no loss of precursor is observed, (3) the metal loading can be fixed and (4) the metal deposit location can be oriented.

References

[1] D.L. Feldheim, C.A. Foss, Metal Nanoparticles Synthesis, Characterization and Applications, Dekker M, New York, 2002.
[2] G. Schmid (Ed.), Nanoparticles: From Theory to Application, Wiley-VCH, Weinheim, 2004.
[3] A. Gual, M. Rosa Axet, K. Philippot, B. Chaudret, A. Denicourt-Nowicki, A. Roucoux, S. Castillón, C. Claver, Chem. Commun., in press, doi:10.1039/B802316F4.
[4] D. Astruc (Ed.), Nanoparticles and Catalysis, Wiley-VCH, Weinheim, 2008.
[5] S. Jansat, M. Gómez, K. Philippot, G. Muller, E. Guiu, C. Claver, S. Castillon, B. Chaudret, J. Am. Chem. Soc. 126 (2004) 1592–1593.
[6] J.G. Vries, C.J. Elsevier (Eds.), The Handbook of Homogeneous Hydrogenation, Wiley-VCH, 2007.
[7] I. Favier, S. Massou, E. Teuma, K. Philippot, B. Chaudret, M. Gómez, Chem. Commun. (2008) 3296–3298.
[8] B.L. Cushing, V.L. Kolesnichenko, C.J. O'Connor, Chem. Rev. (2004) 3893–3946.
[9] V. Mévellec, A. Roucoux, Inorg. Chim. Acta 357 (10) (2004) 3099–3103.
[10] V. Mévellec, A. Nowicki, A. Roucoux, C. Dujardin, P. Granger, E. Payen, K. Philippot, New J. Chem. 30 (8) (2006) 1214–1219.
[11] M. Hemati, D. Steinmetz, B. Chaudret, K. Philippot, Fabrication de catalyseur d'un nouveau type par imprégnation en lit fluidisé, Brevet EPI-PCT/FR 02/01795, 2001.
[12] L. Barthe, Synthèse et dépôt de nanoparticules métalliques dans un support poreux par imprégnation en voies sèche dans un lit fluidisé : élaboration de catalyseurs supportés, PhD thesis, INP Toulouse, 2007.
[13] L. Barthe, S. Desportes, M. Hemati, K. Philippot, B. Chaudret, Chem. Eng. Res. Des. 85 (A6) (2007) 1–11.
[14] N.T. Burdine, Petroleum Trans. Am. Inst. Mining Eng. 198 (1953) 71–77.
[15] S. Desportes, Imprégnation en voie sèche en lit fluidisé, application à la synthèse de catalyseurs supportés, PhD thesis, INP Toulouse, 2005.
[16] J. Schulz, A. Roucoux, H. Patin, Chem. Eur. J. 6 (4) (2000) 618–624.
[17] J. Schulz, S. Levigne, A. Roucoux, H. Patin, Adv. Synth. Catal. 344 (3) (2002) 266–269.
[18] D. Barby, in: G.D. Parfitt, K.S.W. Sing (Eds.), Characterization of Powder Surfaces, Academic Press, London, 1976.
[19] M. Boutros, F. Launay, A. Nowicki, T. Onfroy, V. Herledan-Sommer, A. Roucoux, A. Gédeon, J. Mol. Catal. A: Chem. 259 (2006) 91.